

Adaptive interaction driven by the learning effect in the spatial prisoner's dilemma

Jiaqi Li(李佳奇), Jianlei Zhang(张建磊), and Qun Liu(刘群)

Citation: Chin. Phys. B, 2024, 33 (**3**): 030202. DOI: 10.1088/1674-1056/acf702
Journal homepage: http://cpb.iphy.ac.cn; http://iopscience.iop.org/cpb

What follows is a list of articles you may be interested in

Effect of conformity on evolution of cooperation in a coordination game

Xianjia Wang(王先甲) and Tao Wang(王饕)
Chin. Phys. B, 2023, 32 (**10**): 100202. DOI: 10.1088/1674-1056/acd9c2

Inference of interactions between players based on asynchronously updated evolutionary game data

Hong-Li Zeng(曾红丽), Bo Jing(景涛), Yu-Hao Wang(王于豪), and Shao-Meng Qin(秦绍萌)
Chin. Phys. B, 2023, 32 (**8**): 080201. DOI: 10.1088/1674-1056/acc7fd

Evolution of donations on scale-free networks during a COVID-19 breakout

Xian-Jia Wang(王先甲) and Lin-Lin Wang(王琳琳)
Chin. Phys. B, 2022, 31 (**8**): 080204. DOI: 10.1088/1674-1056/ac4651

The evolution of cooperation in public good game with deposit

Xian-Jia Wang(王先甲), Wen-Man Chen(陈文嫚)
Chin. Phys. B, 2019, 28 (**8**): 080201. DOI: 10.1088/1674-1056/28/8/080201

Evolutionary game dynamics of combining the Moran and imitation processes

Xian-Jia Wang(王先甲), Cui-Ling Gu(顾翠伶), Shao-Jie Lv(吕少杰), Ji Quan(全吉)
Chin. Phys. B, 2019, 28 (**2**): 020203. DOI: 10.1088/1674-1056/28/2/020203

Adaptive interaction driven by the learning effect in the spatial prisoner's dilemma

Jiaqi Li(李佳奇)[1,†], Jianlei Zhang(张建磊)[2], and Qun Liu(刘群)[1]

[1] *Institute of Intelligent Information, Hexi University, Gansu* 734000, *China*
[2] *College of Artificial Intelligence, Nankai University, Tianjin* 300350, *China*

(Received 4 June 2023; revised manuscript received 22 August 2023; accepted manuscript online 6 September 2023)

We propose a computing model in which individuals can automatically adjust their interaction intensity with their mentor according to the learning effect. This model is designed to investigate the cooperative dynamics of the spatial prisoner's dilemma. More specifically, when the cumulative payoff of a learner is more than his reference earning, he will strengthen his interaction with his mentor; otherwise, he will reduce it. The experimental results indicate that this mechanism can improve the emergence of cooperation in a networked population and that the driving coefficient of interaction intensity plays an important role in promoting cooperation. Interestingly, under a certain social dilemma condition, there exists a minimal driving coefficient that leads to optimal cooperation. This occurs due to a positive feedback effect between the individual's satisfaction frequency and the number of effective neighbors. Moreover, we find that the experimental results are in accord with theoretical predictions obtained from an extension of the classical pair-approximation method. Our conclusions obtained by considering relationships with mentors can provide a new perspective for future investigations into the dynamics of evolutionary games within structured populations.

Keywords: self-adapting interaction, evolutionary game, mentor, spatial prisoner's dilemma

PACS: 02.50.Le, 89.75.Fb, 05.45.Pq **DOI:** 10.1088/1674-1056/acf702

1. Introduction

It can be seen from Darwin's theory of evolution that competition among individuals leads to the evolution of species and that any altruistic behavior will quickly disappear over time.[1,2] However, numerous real-world scenarios deviate from Darwinian theory. For example, the emergence of cooperation is often found in biological systems as well as social systems, especially among animal or human communities.[3–7] To investigate such a curious and confused question, a large number of researchers have devoted themselves to researching the essential reason for cooperation behavior between self-interested individuals.[8–10] It is worth highlighting that evolutionary game theory is a very effective tool to account for the origin and persistence of cooperation, by using some game-theoretical models of different scenarios. Interestingly, two-player-two-strategy game models are widely used to analyze bewilderment,[11–16] especially the prisoner's dilemma game (PDG), because it reflects the most unfavorable conditions for cooperation.

About three decades ago, scholars often assumed that a population structure is infinite and well-mixed; that is to say, the likelihood of interaction between two arbitrary individuals is the same. However, in a real system, the contact between individuals is neither fully coupled nor completely random. Nowak and May published a seminal work describing network reciprocity[17,18] and demonstrated that a two-dimensional square lattice can effectively support cooperation in the PDG. Along this research line, some research works have focused on different topologies, including the famous small-world network and one with a scale-free feature.[19,20] Furthermore, some social factors, such as reward and punishment,[21,22] reputation,[23–26] aspiration,[27] tolerance,[28] teaching activity,[29] rationality,[30,31] memory,[32–34] and emotion,[35] have been investigated in the spatial structure. In recent years, many scholars set about studying the reaction of evolutionary game dynamics to networks, especially involving restructuring partnerships[36] and migration.[37] Additionally, the cooperative dynamics of multi-layer networks have also attracted extensive attention.[38–40]

In most of the works described above, scholars generally assumed that individuals undoubtedly interact with their respective neighbors. However, real life tells us that individuals do not always have positive contact with their neighbors and discontinuous contact is more consistent with real situations. In view of this, some scholars put forward various random interaction mechanisms to study the cooperative dynamics in a structured population.[8,41,42] In brief, all these works enrich the knowledge of cooperative dynamics in more realistic environments. Despite this, it should be pointed out that the interaction desire between selfish individuals is not symmetrical and an individual's interaction desire with his mentor should be closely related to the mentor's influence on him. Inspired by these factors, we study the cooperative dynamics in a network by adaptively adjusting the interaction intensity with mentors.

[†]Corresponding author. E-mail: lijiaqi006@126.com

© 2024 Chinese Physical Society and IOP Publishing Ltd

The remainder of this article is organized as follows. In Section 2, we briefly introduce related background knowledge, including the networked population structure and the spatial PDG, as well as the constraint interaction condition between individuals. Section 3 describes our model in detail. The results are arranged in Section 4, and Section 5 gives our conclusions.

2. Related knowledge

2.1. Population structure and the spatial PDG

We first introduce population structure and the spatial PDG. Nodes and edges on the network represent the individuals and the interactive relationship between individuals, respectively. Next, we attach a reversible direction to each edge and the weights in the direction denote the strength of interaction with each other (the probability of interaction). For example, for two arbitrary individuals (say x and y) who have a paired relationship on the network, x will willingly interact with his partner y by the unilateral interaction strength $W_{x\rightharpoonup y}$, and y will do that with x by the corresponding interaction strength $W_{y\rightharpoonup x}$. Under such a framework, only when both parties successfully send interaction intentions to an opponent can they participate in the game. Furthermore, we use two unit vectors to represent the strategies that the individual is likely to choose (cooperation strategy C and defection strategy D are represented by $S_x(t)=[1,0]^{\mathrm{T}}$ and $S_x(t)=[0,1]^{\mathrm{T}}$, respectively). Generally, the two-player-two-strategy social dilemma models are described by the payoff matrix[17,43]

$$M=\begin{array}{c} \\ \mathrm{C} \\ \mathrm{D} \end{array}\begin{array}{c} \begin{array}{cc} \mathrm{C} & \mathrm{D} \end{array} \\ \begin{pmatrix} R & S \\ T & P \end{pmatrix} \end{array}. \tag{1}$$

In Eq. (1), mutual cooperation and mutual defection result in the payoffs R and P, respectively. However, when the cooperator encounters the defector, the former obtains the payoff S, while the latter gets T. For the PDG, these payoffs obey the ranking $T>R>P>S$ and satisfy the constraint $2R>T+S$. For simplicity, we set $T=b$, $R=1$, and $P=S=0$, where the parameter b ($1<b<2$) represents the temptation value of betrayal.

2.2. Interaction condition

According to context, the constraint interaction condition between x and his neighbor y at time t step is described by

$$I_{x,y}(t)=\begin{cases} 1 & (E_{x\rightharpoonup y}=1 \text{ and } E_{y\rightharpoonup x}=1), \\ 0 & (\text{others}). \end{cases} \tag{2}$$

In Eq. (2), $I_{x,y}(t)$ denotes the logical outcome of whether or not there is a successful interaction; $E_{x\rightharpoonup y}$ denotes the event that individual x successfully transmits the interaction intention with $W_{x\rightharpoonup y}$ to his neighbor y. Where, the term for successful transmission (hereinafter, abbreviated as success) means y receives the interaction signal that comes from x. Obviously, the probability that y receives the signal will be gradually increased with the increasing value of $W_{x\rightharpoonup y}$. In addition, if the signal is successfully transmitted, the logical result of the event $E_{x\rightharpoonup y}$ is equal to "1"; otherwise it is "0". Similarly, event $E_{y\rightharpoonup x}$ has the same meanings as $E_{x\rightharpoonup y}$, that is,

$$E_{x\rightharpoonup y}(t)=\begin{cases} 1 & (\text{success}), \\ 0 & (\text{failure}), \end{cases} \quad E_{y\rightharpoonup x}(t)=\begin{cases} 1 & (\text{success}), \\ 0 & (\text{failure}). \end{cases} \tag{3}$$

Only when the two independent interaction events both occur at the same time can they (x and y) participate in the game.

3. Model

There are three stages in each round of the game: interaction, modification of interaction strength and strategic learning.

First, each individual (say x) interacts with his neighbors simultaneously with the same strategy and the corresponding interaction strength and calculates his accumulated earning in the current round

$$\pi_x(t)=\sum_{y\in N_x} I_{x,y}(t)S_x^{\mathrm{T}}(t)MS_y(t), \tag{4}$$

where the symbol N_x denotes x's neighbor set.

Next, it is necessary to define two basic concepts to facilitate description of the revision rule of the interaction intensity.

Definition 1 (mentor) If individual x successfully learns the previous strategy $S_y(t-1)$ of his neighbor y, then y will be regarded as x's mentor at present. In addition, x's mentor is likely to be constantly replaced as the system evolves.

Definition 2 (reference payoff) We treat the cumulative payoff $\pi_x(t-1)$ of individual x, which is the one he has obtained in the previous round, as his reference payoff at time t step.

Entering the second stage after interaction, the individual x is likely to spontaneously adjust the interaction intensity from himself to his mentor (say y) according to the difference between x's cumulative payoff and reference payoff, and the regulated result will be regarded as the interaction intensity from himself to y in the next round

$$W_{x\rightharpoonup y}(t+1)=W_{x\rightharpoonup y}(t)+\Delta W_{x\rightharpoonup y}. \tag{5}$$

As seen from Eq. (5), $\Delta W_{x\rightharpoonup y}$ signifies the modified increment of interaction strength from x to y, and

$$\Delta W_{x\rightharpoonup y}=\delta\times\tanh\left[\pi_x(t)-\pi_x(t-1)\right], \tag{6}$$

where parameter δ ($0\le\delta\le 1$) represents the driving coefficient of interaction intensity, which means the speed of change

of interaction intensity. When $\delta = 0$, the intensity of interaction between individuals is invariably decided by initialization. When $\delta > 0$, the interactive relationship between individuals is going to change continuously with time and it becomes faster and faster with the gradual increase of the driving coefficient. In addition, the modified increment of the interactive relationship is determined by the hyperbolic tangent function, because this kind of function can vividly depict the dynamic change of an interpersonal relationship. According to the context, when x's cumulative income obtained by imitating the strategy of his mentor y is more than the reference payoff $[\pi_x(t) > \pi_x(t-1)]$, x is satisfied and he will enhance the interaction with y. Conversely, x is dissatisfied with y in cases of $\pi_x(t) < \pi_x(t-1)$ and he will weaken the interaction. Especially, $W_{x\rightharpoonup y}(t+1) = W_{x\rightharpoonup y}(t)$ when the difference is equal to 0.

Finally, it is necessary for every individual to learn from his neighbor in order to get a higher payoff in the next round. We adopt the widely used Fermi function for the updating rule of an individual strategy.[44] Namely, an individual x picks one of his neighbors (say y) at random and whether y can act as x's new mentor depends on the probability

$$f[\pi_x(t) - \pi_y(t)] = \frac{1}{1 + e^{[\pi_x(t) - \pi_y(t)]/K}}. \tag{7}$$

Here K represents the noise intensity ($K \geq 0$) involved in the strategy-updating process. In this article, we principally study how the driving coefficient δ of the interaction intensity affects the evolution of cooperation in the spatial PDG.

4. Results

Experiments are carried out on a two-dimensional square lattice. Different from the previous networked population, we use a directed and weighted network of $N \times N$ size to describe the population structure. Initially, the value of the unidirectional interaction strength is evenly distributed between 0 and 1. It should be noted that owing to the dynamic changes within the system, the interaction strength may exhibit unusual phenomena, such as values that are either less than or equal to zero or greater than one. To avoid the occurrence of these anomalies, we control the amplitude of unidirectional interaction strength between 0 and 1. In addition, each individual on the network is stochastically initialized as either C or D with an equal probability of 0.5. To obtain the density of cooperation ρ_c during the steady-state operation of system, we compute the value of ρ_c by averaging the last m rounds of the whole T rounds and each data point is plotted in the following figures as the average value for n times independent experiments.

4.1. Influence of the temptation value

We first investigate the density of cooperation ρ_c as a function of the temptation value b for different driving coefficient δ, as shown in Fig. 1. As can be seen from Fig. 1(a), different from the effect of a spatial game under fixed interaction strength ($\delta = 0$), ρ_c is significantly enhanced and cooperators can even attain the absolute superiority of dominating the whole population when considering the self-adapting interaction driven by the learning effect ($\delta > 0$). More specifically, when $\delta = 0.1$, the density of cooperation is obviously higher than that for the conventional mode ($\delta = 0$) and the density of cooperation increases with increasing δ. Moreover, when $\delta = 0.1$, the critical value for the disappearance of cooperation, b_{cr}, increases to 1.075. In contrast, it is only close to 1.045 for the conventional mode. Subsequently, b_{cr} is gradually enhanced with the increase of δ.

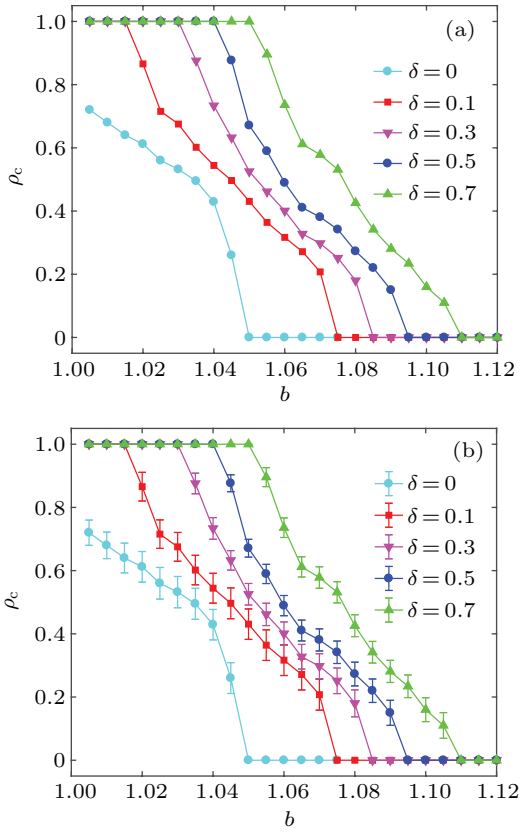


Fig. 1. Density of cooperation ρ_c as a function of the temptation value b for different driving coefficient δ. (a) The results obtained by simulations; (b) the error bar of each data point. The evolutionary PDG is performed on a 100×100 directed and weighted square lattice. As can be seen from panel (a), compared with the traditional mode ($\delta = 0$), density of cooperation is significantly enhanced and cooperators can even attain the absolute superiority of dominating the whole population when considering the self-adapting interaction driven by the learning effect ($\delta > 0$). Some other relevant parameters: $K = 0.1$, $m = 2 \times 10^3$, $T = 10^4$ (even 10^5) and $n = 100$.

In addition, we survey the extent to which the density of cooperation obtained in each experiment deviates from the mean value of density of cooperation obtained in multiple experiments (see Fig. 1(b)). The calculation method of error quantity τ is as follows:

$$\tau = \sqrt{\frac{1}{n}\sum_{i=1}^{n}(\rho_i - \rho_c)^2}. \tag{8}$$

In Eq. (8), ρ_c denotes the density of cooperation, which is the average value obtained by n times independent experiments; the signal ρ_i $(i = 1, 2, \ldots, n)$ represents the density of cooperation obtained in each experiment. According to statistics, although there are deviations between ρ_i and ρ_c $(0 < \rho_c < 1)$, the length of the error bar for each data point is fairly small. For example, when $\delta = 0.3$ and $b = 1.05$, the value of τ is roughly equal to 0.03, which means that the result obtained through each experiment is almost always around the mean value. In brief, these data points in Fig. 1 perfectly represent the relationship between ρ_c and b for different values of δ.

It is worth noting that the above results are obtained under the assumption that the noise intensity K is set to 0.1,[45,46] but it is just a special case. Therefore, it is necessary to investigate if cooperation density ρ_c is affected by the temptation value b for different values of K. After experiments, we find that it is more conducive to cooperation when the noise intensity is controlled within a certain range. Specifically speaking, for a fixed value of b, when $K = 0$, all cooperators are wiped out by defectors ($\rho_c = 0$); nevertheless, ρ_c will rise rapidly as long as the value of K is increased slowly. Unfortunately, once the value of K exceeds 1.8, ρ_c will begin to decrease as K continues to increase. Furthermore, the extinction threshold of cooperation (b_{cr}) is also gradually enhanced with the increase of K $(0 \leq K \leq 1.8)$. These phenomena indicate that cooperation will be inhibited when the noise is too low or too high, while the appropriate noise intensity is beneficial to cooperation.

4.2. Role of the driving coefficient

To accurately quantify the effects of self-adapting interaction driven by learning on cooperation, we study the relationship between the density of cooperation and the driving coefficient for different temptation values, as shown in Fig. 2. Obviously, for each fixed value of b, we can observe that the density of cooperation increases monotonously with an increasing value of δ. Interestingly, for each small or moderate temptation value (such as $b = 1.02$ and $b = 1.05$), we notice that the cooperators have the absolute advantage of being able to dominate the whole population as long as δ exceeds a critical threshold. That is, in this social dilemma, there is a small driving coefficient $\delta_{\min}$ that can make all individuals in the population reach the saturation state of cooperation. However, for a large temptation value (such as $b = 1.08$), although cooperators do not have the advantage of dominating the whole population, there is still a small driving coefficient $\delta_{\min}$ that can provide a moderate environment for the survival of cooperators. More clearly,

$$\left\{\delta \middle| \delta_{\min} \leq \delta \leq 1\right\} = \arg\max_{\delta \in [0,1]} \rho_c. \tag{9}$$

Similarly, we also check the error bars of the above data points (see Fig. 2(a)). As you can see, the length of the error bar for each data point is small. Just like the meaning expressed earlier for the error bar, the shorter the error bar, the smaller the difference between the density of cooperation obtained from per experiment and the mean. Curiously, the length of the error bar gradually decreases with increasing the driving coefficient δ for a fixed b. We believe that the reason for this phenomenon is that the randomness of interactions between individuals decreases as δ increases. We further consider the effect of noise intensity K on the density of cooperation ρ_c. The results show that the appropriate noise can also improve the cooperation in the population and the value of $\delta_{\min}$ decreases with the increase of noise in a certain range of noise.

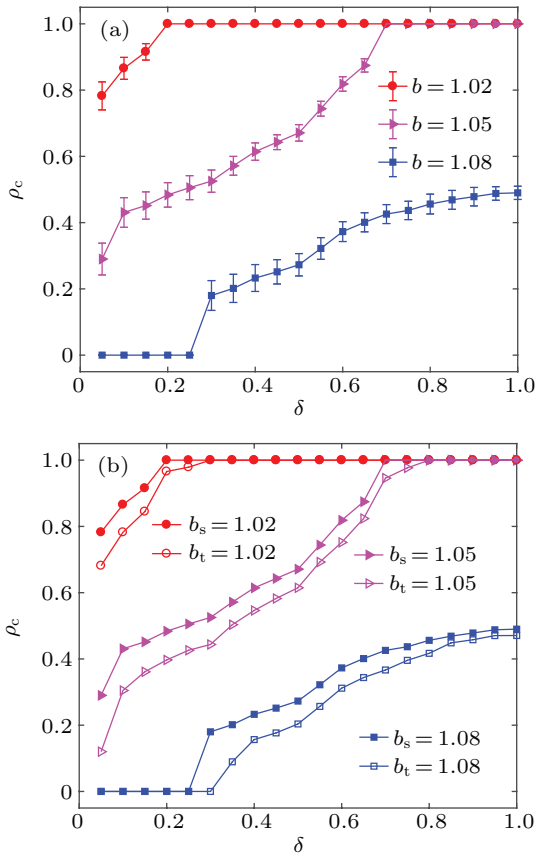


Fig. 2. The relationship between the density of cooperation ρ_c and the driving coefficient δ for different temptation values. (a) The results and the corresponding error bar. (b) The contrast between the theoretical analysis result and numerical simulation result. Obviously, for each fixed value of b, there is the smallest driving coefficient $\delta_{\min}$ which can provide the moderate environment for the spread of cooperative behavior. Furthermore, the results are basically coincident between theoretical analysis (b_t) by the extended pair approximation and numerical simulation (b_s), although there are some subtle differences. Some other relevant parameters: $N = 100$, $K = 0.1$, $m = 2 \times 10^3$, $T = 10^4$ (even 10^5) and $n = 100$.

The following is an extension of the pair-approximation method[47] and we apply it to confirm the numerical simulation results showing that the density of cooperation changes with the driving coefficient. In Fig. 3, we randomly choose an individual whose strategy is x to learn strategy by comparing his accumulated payoff with a randomly chosen partner with

strategy y.

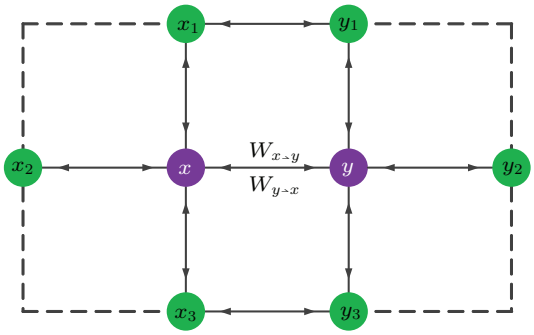


Fig. 3. Concentrating on the pairwise two individuals with strategy x and strategy y on the directed and weighted square lattice shows the relevant configuration for the extended pair approximation. The change of pair configuration probabilities $p_{x,y\rightarrow y,y}$ can be determined based on this structure. For clarity, we only write the value of the unilateral interaction intensity ($W_{x\rightarrow y}$ and $W_{y\rightarrow x}$) between x and y.

We first calculate the average amplitude of interactive strength for each strategy combination to obtain the cumulative benefits for individuals. According to the payoff matrix of the PDG, we just need to figure out the average amplitude of interactive strength between the cooperators (denoted by $W_{\mathrm{c,c}}^{\mathrm{av}}$), as well as between the cooperators and defectors (denoted by $W_{\mathrm{c,d}}^{\mathrm{av}}$). We use the following calculation method:

$$W_{\mathrm{c,c}}^{\mathrm{av}} = \frac{\sum_n \sum_m \sum I_{\mathrm{c,c}}}{\sum_n \sum_m \sum (I_{\mathrm{c,c}} + \bar{I}_{\mathrm{c,c}})}, \tag{10}$$

$$W_{\mathrm{c,d}}^{\mathrm{av}} = \frac{\sum_n \sum_m \sum I_{\mathrm{c,d}}}{\sum_n \sum_m \sum (I_{\mathrm{c,d}} + \bar{I}_{\mathrm{c,d}})}. \tag{11}$$

In Eqs. (10) and (11), the symbol $\sum I_{x,y}$ means the pair quantity of successful interactions between individuals in each round. More explicitly, $\sum I_{\mathrm{c,c}}$ denotes the pair quantity of successful interactions between cooperators in each round, $\sum I_{\mathrm{c,d}}$ denotes the one between cooperator and defector. We already know that the logical outcome will be equal to "0" if interactions fail for paired individuals; in this case, the inverse operation of the logical result will equal "1", that is, $\bar{I}_{x,y} = 1$. Therefore, $\sum (I_{\mathrm{c,c}} + \bar{I}_{\mathrm{c,c}})$ means the pair quantity regardless of whether or not there is successful interaction between cooperators. Similarly, $\sum (I_{\mathrm{c,d}} + \bar{I}_{\mathrm{c,d}})$ has the same meanings as $\sum (I_{\mathrm{c,c}} + \bar{I}_{\mathrm{c,c}})$. After n times independent experiments, we define the average amplitude of interaction strength between cooperators as the proportion of successful interactions between cooperators to the total number of interactions, regardless of whether such interactions were successful or not. The average amplitude of interactive strength between cooperators and defectors can be also obtained by a similar method. Incidentally, we can get $W_{\mathrm{d,c}}^{\mathrm{av}} = W_{\mathrm{c,d}}^{\mathrm{av}}$ according to the symmetry.

We imagine y and x as a cooperator and a defector, respectively, and then the accumulated income of the cooperator for different configurations is

$$\pi_{\mathrm{c}}\left(y_1, y_2, y_3, W_{\mathrm{c,c}}^{\mathrm{av}}\right) = W_{\mathrm{c,c}}^{\mathrm{av}} \times n_{\mathrm{c}}\left(y_1, y_2, y_3\right) \times 1, \tag{12}$$

here $n_{\mathrm{c}}(y_1, y_2, y_3)$ represent the number of cooperators in the neighbors y_1, y_2, y_3. Likewise, we can also imagine that if y is a defector and x is a cooperator, then the accumulated income of the defector for different configurations is

$$\pi_{\mathrm{d}}\left(y_1, y_2, y_3, W_{\mathrm{d,c}}^{\mathrm{av}}\right) = W_{\mathrm{d,c}}^{\mathrm{av}} \times \left[n_{\mathrm{c}}(y_1, y_2, y_3) + 1\right] \times b. \tag{13}$$

Whenever x succeeds in learning y's strategy, the pair configuration probabilities will change, thus generating a group of differential equations that determine the evolution of the system

$$\begin{aligned}
\dot{p}_{\mathrm{c,c}} = & \sum_{x_1,x_2,x_3} \left[n_{\mathrm{c}}(x_1, x_2, x_3) + 1\right] p_{\mathrm{d},x_1} p_{\mathrm{d},x_2} p_{\mathrm{d},x_3} \\
& \times \sum_{y_1,y_2,y_3} p_{\mathrm{c},y_1} p_{\mathrm{c},y_2} p_{\mathrm{c},y_3} f(\theta_1 - \theta_3) \\
& + \sum_{x_1,x_2,x_3} \left[-n_{\mathrm{c}}(x_1, x_2, x_3)\right] p_{\mathrm{c},x_1} p_{\mathrm{c},x_2} p_{\mathrm{c},x_3} \\
& \times \sum_{y_1,y_2,y_3} p_{\mathrm{d},y_1} p_{\mathrm{d},y_2} p_{\mathrm{d},y_3} f(\theta_2 - \theta_4),
\end{aligned} \tag{14}$$

$$\begin{aligned}
\dot{p}_{\mathrm{c,d}} = & \sum_{x_1,x_2,x_3} \left[1 - n_{\mathrm{c}}(x_1, x_2, x_3)\right] p_{\mathrm{d},x_1} p_{\mathrm{d},x_2} p_{\mathrm{d},x_3} \\
& \times \sum_{y_1,y_2,y_3} p_{\mathrm{c},y_1} p_{\mathrm{c},y_2} p_{\mathrm{c},y_3} f(\theta_1 - \theta_3) \\
& + \sum_{x_1,x_2,x_3} \left[n_{\mathrm{c}}(x_1, x_2, x_3) - 2\right] p_{\mathrm{c},x_1} p_{\mathrm{c},x_2} p_{\mathrm{c},x_3} \\
& \times \sum_{y_1,y_2,y_3} p_{\mathrm{d},y_1} p_{\mathrm{d},y_2} p_{\mathrm{d},y_3} f(\theta_2 - \theta_4),
\end{aligned} \tag{15}$$

where

$$\begin{cases}
\theta_1 = \pi_{\mathrm{c}}(y_1, y_2, y_3, W_{\mathrm{c,c}}^{\mathrm{av}}), \\
\theta_2 = \pi_{\mathrm{d}}(y_1, y_2, y_3, W_{\mathrm{d,c}}^{\mathrm{av}}), \\
\theta_3 = \pi_{\mathrm{d}}(x_1, x_2, x_3, W_{\mathrm{d,c}}^{\mathrm{av}}), \\
\theta_4 = \pi_{\mathrm{c}}(x_1, x_2, x_3, W_{\mathrm{c,c}}^{\mathrm{av}}),
\end{cases} \tag{16}$$

and $\pi_{\mathrm{d}}\left(x_1, x_2, x_3, W_{\mathrm{d,c}}^{\mathrm{av}}\right)$ and $\pi_{\mathrm{c}}\left(x_1, x_2, x_3, W_{\mathrm{c,c}}^{\mathrm{av}}\right)$ denote respectively as

$$\pi_{\mathrm{d}}\left(x_1, x_2, x_3, W_{\mathrm{d,c}}^{\mathrm{av}}\right) = W_{\mathrm{d,c}}^{\mathrm{av}} \times \left[n_{\mathrm{c}}\left(x_1, x_2, x_3\right) + 1\right] \times b, \tag{17}$$

$$\pi_{\mathrm{c}}\left(x_1, x_2, x_3, W_{\mathrm{c,c}}^{\mathrm{av}}\right) = W_{\mathrm{c,c}}^{\mathrm{av}} \times n_{\mathrm{c}}\left(x_1, x_2, x_3\right) \times 1. \tag{18}$$

Obviously, the common factor $2p_{\mathrm{c,d}}/(p_{\mathrm{c}}^3 p_{\mathrm{d}}^3)$ has been omitted in Eqs. (14) and (15). Even so, the equilibrium of system remains unaffected because the common factor only serves as nonlinear transformations in timescale.

Subsequently, combining the symmetry property $p_{\mathrm{d,c}} = p_{\mathrm{c,d}}$ and the constraint condition $p_{\mathrm{c,c}} + p_{\mathrm{d,c}} + p_{\mathrm{c,d}} + p_{\mathrm{d,d}} = 1$, we can obtain the density of cooperation in the population $\rho_{\mathrm{c}} = p_{\mathrm{c,c}} + p_{\mathrm{c,d}}$.

Additionally, for the extended version of the pair approximation, it will be simplified to the traditional mode if the interaction intensity between individuals evolves to a saturation state ($W_{\mathrm{c,c}}^{\mathrm{av}} = W_{\mathrm{c,d}}^{\mathrm{av}} = W_{\mathrm{d,c}}^{\mathrm{av}} = W_{\mathrm{d,d}}^{\mathrm{av}} = 1$).

As can be seen from Fig. 2(b), the results are basically coincident between theoretical analysis by the extended pair

approximation and numerical simulation, although there are some subtle differences. However, we think that the differences between them may be because we do not consider the effect of spatial clusters in the extended pair approximation method, especially the cooperative cluster. Despite this fact, our extension method also successfully verifies the simulation results and qualitatively reflects the role of self-adapting interaction driven by learning.

4.3. Dynamics analysis

Next, we collect some typical evolution snapshots of individuals on the network to improve our comprehension of the mechanism of adaptive interaction driven by the learning effect, as shown in Fig. 4. To visualize different states of individuals at each time step, we adopt several colors to represent individual behavior. Wine, dark green and blue represent the old cooperators, the old defectors and the isolators, respectively. Correspondingly, red and green denote the new cooperators (from other states to cooperation) and the new defectors (from other states to betrayal), respectively. We can also judge the equilibrium state of the system from the perspective of evolution snapshots by setting an individual's color in this way. For example, when the proportion of the new cooperators is almost equal to that of the new defectors in the population, we can consider that the system probably arrives at the equilibrium state.

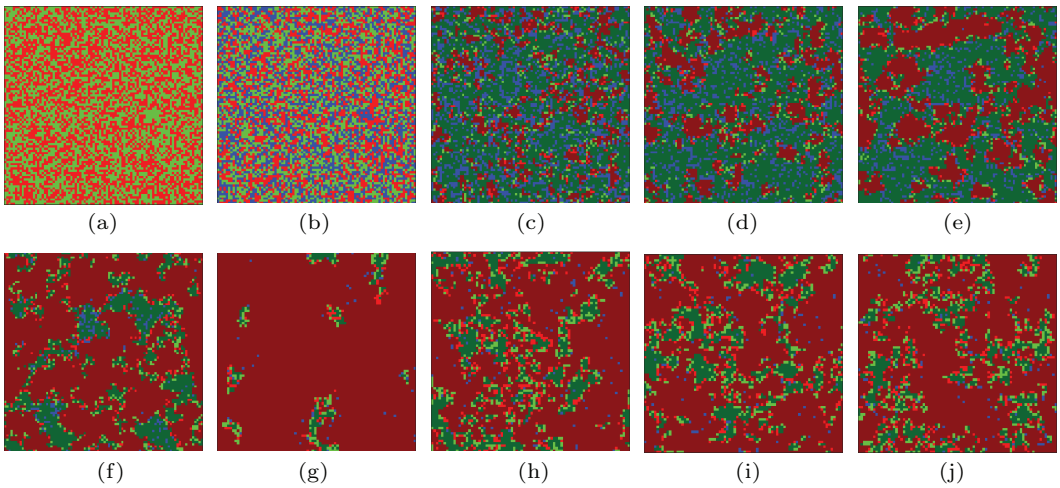


Fig. 4. Some typical evolution snapshots of an individual's states on a square lattice for a moderate level of temptation ($b = 1.05$) and an appropriate driving coefficient ($\delta = 0.6$) at several representative time steps. Wine, dark green and blue represent the old cooperators, the old defectors and the isolators, respectively. Correspondingly, red and green denote the new cooperators (from other individual states to cooperation) and the new defectors (from other individual states to betrayal), respectively. From (a) to (j), the collected time steps are 0, 1, 20, 50, 100, 200, 300, 500, 1000 and 3000, respectively. Other relevant arguments: $N = 100$, $K = 0.1$.

Before the system runs, each individual in the population is defined as a cooperator (red) or a defector (green) with the fixed probability 0.5, so the network is evenly filled with two different types of individuals (Fig. 4(a)). Nevertheless, once the system is up and running, about 33% of the individuals are at high risk of losing contact with their neighbors and they exist evenly in the population as isolators (blue) owing to very weak interactions that are decided by initialization (Fig. 4(b)). It should be noted that we consider cooperators and defectors, whether in Fig. 4(a) or in Fig. 4(b), as the neonatal state in the corresponding time step. Therefore, we still use red and green to represent cooperators and defectors, respectively. In the first stage of system operation, the vast majority of individuals tend to choose the betrayal strategy in order to satisfy their own desires. In such an environment filled with selfishness, defection clusters (denoted by Ω_{D}) quickly form through the constant gathering of defectors. Unfortunately, some of the traitors located within Ω_{D} will be quarantined, which is a heavy price to pay for selfish interests at the expense of friendship. Despite that, there are still a few loyal collaborators who survive by forming close alliances (called cooperative clusters, denoted by Ω_{C}) (Fig. 4(c)). The scale of Ω_{C} in the initial stage of system evolution is noteworthy. As can be seen from Fig. 4(c), when the system evolves to the end of the primary stage, not only is the number of Ω_{C} small, but also their respective sizes are also small. However, for each Ω_{C}, the partnership between individuals is very friendly because an individual (say x) is likely to be satisfied with his current cumulative returns $[\pi_x(t) > \pi_x(t-1)]$ by studying its cooperative neighbor (say y). This leads to an increase of interaction intensity with his partner y. The more rounds of successful learning there are, the higher the frequency of interaction and the richer the individual x becomes. Furthermore, with the increasing prosperity of individuals within Ω_{C}, the surrounding cooperators are also getting richer. In contrast, a relatively static scene appears within each Ω_{D} because the defectors will gain nothing from their interactions. In other words, within each Ω_{D}, the interactive relation between individuals does not change over time. In this way, the unsuccessful defection group cannot bring any benefit to any of its members, including those individuals on

the border. In such circumstances, opportunistic betrayers located at the boundary of Ω_D easily become cooperators by learning from their relatively affluent cooperation neighbors. Soon afterwards, the less cohesive Ω_D can be easily gradually destroyed by close-knit Ω_C. In addition, the cooperators never stop fulfilling the obligation of rescuing loners. Therefore, the scale of Ω_C is gradually expanded as time passes (from Fig. 4(d) to Fig. 4(f)). Surprisingly, the size of Ω_C does not always increase as the system further evolves. To be specific, at about $t = 300$, the cooperators become almost absolutely dominant in the population because they form huge, interconnected slices through alliances (Fig. 4(g)). However, this favorable situation is only temporary and is closely followed by a very different scene. The defectors renew their attack on the cooperators, which causes Ω_C to shrink gradually in size, while the Ω_D swells gradually (Fig. 4(h)). After a fierce confrontation between collaborators and defectors, the proportion of neonatal cooperators is almost equal to that of the neonatal defectors (from Fig. 4(i) to Fig. 4(j)), which means that the system has entered a stable state.

In the following, we will explain more clearly the dynamics of the evolution of these typical snapshots by looking at the average payoff (AP) of individuals with different types, as shown in Fig. 5. As shown in Fig. 5(a), although the fact that the AP of cooperators (denoted by AP_c) is almost always less than that of defectors (denoted by AP_d) during the primary stage ($t < 100$), the difference between them gradually decrease over time. In other words, the probability that C learns from D ($f[\pi_C(t) - \pi_D(t)]$) is almost always higher than the probability that D learns from C ($f[\pi_D(t) - \pi_C(t)]$) during this period, but the probability of a mutual switch between C and D is getting gradually closer. This means Ω_C can be formed gradually during the initial phase of the system. Owing to the fact that Ω_C can enhance the competitiveness of their circumjacent cooperators, the exploitation of collaborators by traitors will be effectively restrained. Furthermore, with the gradual enhancement of circumjacent cooperators' competitiveness, they will have more and more opportunities to win over isolators. Therefore, throughout the process of system evolution before $t = 100$, the density of cooperation changes from a gradual decline at the beginning to a gradual rise later [see Fig. 5(b)]. However, once the value of AP_c exceeds that of AP_d ($t > 100$), the density of cooperation will rise rapidly and gradually reach the uppermost point (about $t = 300$), then quickly fall. For this phenomenon, in our opinion, as Ω_C gradually grows in size, the number of defectors around the Ω_C perhaps is getting less and less. However, the fighting capacity of those defectors is getting stronger and stronger because defectors are probably interacting with more and more cooperators and getting higher and higher payoffs. Unfortunately, the strong counterattack of the betrayers does not achieve great success, although it strikes at the cooperators' absolute dominance over the population. After a period of intense struggle between collaborators and defectors, the system reaches a state of relative equilibrium ($t > 2000$). Note that because isolators are constantly being rescued by cooperators and defectors, the final scenario of system evolution is mainly the coexistence of cooperators and betrayers.

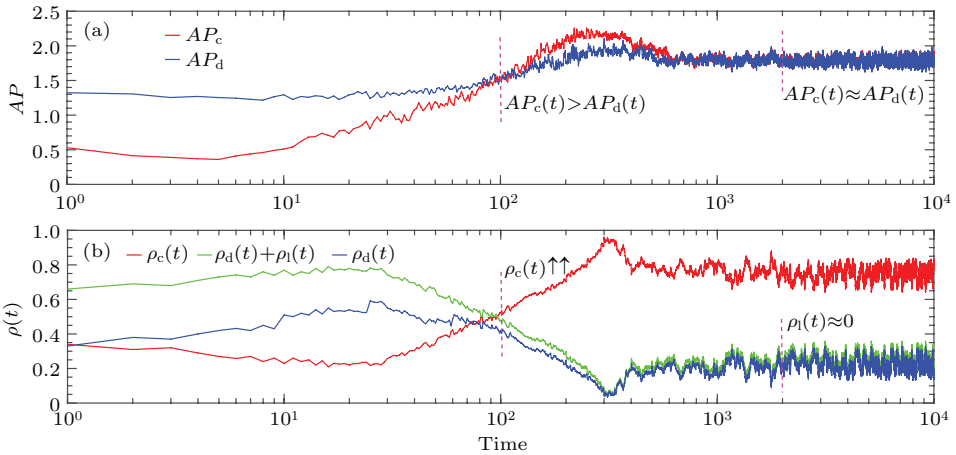


Fig. 5. Dynamic analysis of typical snapshots by looking at the average payoff (AP) of different types of individuals. As can be seen from panel (a), although the fact that the AP of cooperators (AP_c) almost always is less than the one of defectors (AP_d) in the beginning, before long, AP_c not only succeeds in catching up with AP_d, but also surpasses it. With the further evolution of the system, AP_c begins to descend until it arrives at the same level with AP_d. Naturally, the density of cooperation ρ_c (see panel (b)) accordingly follows the trajectory from an initial decline to a gradual increase and then to a steady amplitude. Other relevant parameters: $N = 100$, $K = 0.1$, $b = 1.05$, $\delta = 0.6$, and $T = 10^4$.

Definition 3 (effective neighbor) The adaptive interaction mechanism can be divided into two processes, one is that an individual adaptively selects some neighbors as his interaction objects according to the corresponding interaction intensity, the other is that a game relationship occurs with mutually selected individuals. In doing so, an individual is likely to interact successfully with only some of his neighbors. We treat the partner who actually interacts with individual x as the effective neighbor of x.

Based on the context, we can easily analyze the evolu-

tionary dynamics of interaction intensity. As we know, the interaction intensity between an individual x and its neighbor y is described as

$$W_{x\to y}(t+1) = W_{x\to y}(t) + \delta \times \tanh\left[\pi_x(t) - \pi_x(t-1)\right]. \quad (19)$$

According to Eq. (1), we know that mutual cooperation can result in the equal payoff R for each party; so, when x is located inside the cooperative cluster $\Omega_{\rm C}$, its accumulated payoff should be proportional to the number of effective neighbors

$$\pi_x(t) = R \times |N_x^{\rm e}|, \quad (20)$$

where the signal $|N_x^{\rm e}|$ denotes the number of x's effective neighbors. In this work, we set $R = 1$, thus $\pi_x(t) = |N_x^{\rm e}|$. In doing so, the dynamic change of interaction intensity inside $\Omega_{\rm C}$ becomes

$$W_{x\to y}(t+1) = W_{x\to y}(t) + \delta \times \tanh\left[|N_x^{\rm e}(t)| - |N_x^{\rm e}|(t-1)\right]. \quad (21)$$

Obviously, for an individual located inside $\Omega_{\rm C}$, he likely to be satisfied with his current payoff obtained by learning from his cooperative neighbor, so he will spontaneously enhance the interaction intensity from himself to his mentor, which possibly leads to there being more chances to interact. That is to say, the number of an individual's effective neighbors will increase as time goes on. Furthermore, the higher the satisfaction frequency, the more effective neighbors an individual will have. In turn, the satisfaction frequency increases with the number of effective neighbors. Obviously, a positive feedback effect can occur as an individual's satisfaction frequency and the amount of effective neighbors influence each other. Due to this, the competitiveness of the cooperators located at the boundary can be improved step by step. When the attack force of boundary cooperators is greater than the defense force of boundary defectors, $\Omega_{\rm D}$ will be demolished and opportunistic turncoats can easily evolve into cooperators through learning.

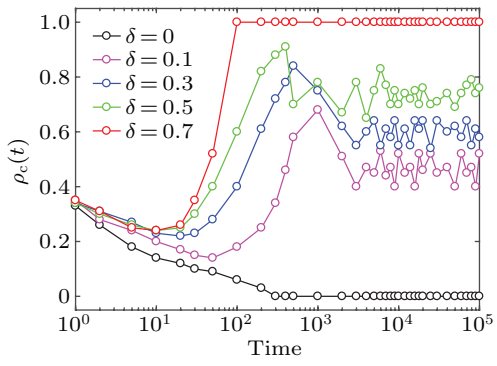


Fig. 6. Dynamic evolution of cooperation density $\rho_{\rm c}(t)$ for different driving coefficients δ. It is shown that solely relying on spatial reciprocity ($\delta = 0$) cannot promote the emergence of cooperation when individuals face a higher temptation to defect. However, for the self-adapting interaction mode driven by learning from neighbors, the scene has changed dramatically and the higher value of δ indicates a stronger positive feedback effect. Relevant parameters: $N = 100$, $K = 0.1$ and $b = 1.05$.

Through the above analysis, it becomes evident that the positive feedback in the system plays a pivotal role in shaping cooperation dynamics. Therefore it is important to gain an in-depth understanding of this phenomenon by investigating the dynamic evolution of cooperation density $\rho_{\rm c}(t)$ for different driving coefficients δ, as shown in Fig. 6. One can see that the cooperators in the population quickly vanish over time in the traditional interaction mode ($\delta = 0$), which means that relying solely on spatial reciprocity cannot promote the emergence of cooperation when individuals are faced with the high temptation value. However, for the self-adapting interaction mode driven by learning from neighbors, the scene changes dramatically. For example, when $\delta = 0.1$, the initial drop of $\rho_{\rm c}(t)$ is quickly controlled, then turns to a period of rapid spreading of cooperators and, finally, arrives at a relatively stable state. Evidently, the essential reason for providing a superior environment for collaborators is the positive feedback effect in the system. In addition, the time required, which is the initial descent of $\rho_{\rm c}(t)$, will be gradually reduced with increasing δ, and the earlier the decline is suppressed, the faster cooperation recovers and the greater the dominance of the cooperators in the population. These phenomena indicate that the higher the value of δ is, the stronger the positive feedback effect will be.

4.4. Robustness of the system under noise

The final but highly significant question pertains to the robustness of the system under the influence of noise intensity in the strategy updating process. On this point, we further investigate the density of cooperation $\rho_{\rm c}$ when influenced by the noise intensity K and the driving coefficient δ, for a smaller (such as $b = 1.02$, left panel) and a bigger (such as $b = 1.10$, right panel) temptation value, as shown in Fig. 7. We divide the $KO\delta$ coordinate plane into three regions so as to be convenient description,

$$\begin{cases} \Theta_{\rm a}^1 = \left\{(K,\delta)\middle|0.0 \le K < 0.1,\ \ 0 < \delta \le 1\right\}, \\ \Theta_{\rm a}^2 = \left\{(K,\delta)\middle|0.1 \le K \le 1.0,\ \ 0 < \delta \le 1\right\}, \\ \Theta_{\rm a}^3 = \left\{(K,\delta)\middle|1.0 < K \le 3.0,\ \ 0 < \delta \le 1\right\}, \end{cases}$$
$$\begin{cases} \Theta_{\rm b}^1 = \left\{(K,\delta)\middle|0.0 \le K < 0.2,\ \ 0 < \delta \le 1\right\}, \\ \Theta_{\rm b}^2 = \left\{(K,\delta)\middle|0.2 \le K \le 0.5,\ \ 0 < \delta \le 1\right\}, \\ \Theta_{\rm b}^3 = \left\{(K,\delta)\middle|0.5 < K \le 3.0,\ \ 0 < \delta \le 1\right\}. \end{cases} \quad (22)$$

For $b = 1.02$, when $(K,\delta) \in \Theta_{\rm a}^1$, cooperators are in a state of extinction. Namely, when $0 \le K < 0.1$, the cooperators are completely gone regardless of the value of δ. When $(K,\delta) \in \Theta_{\rm a}^2$, for an arbitrary value of δ, $\rho_{\rm c}$ is promptly enhanced, and even reaches a saturation condition with the slight increase of K. However, as K further increases, $\rho_{\rm c}$ starts

to decrease gradually when $(K,\delta) \in \Theta_a^3$. These phenomena highlight the presence of an optimal noise environment that can most effectively facilitate the propagation of cooperation, aligning with the outcome that appropriate noise levels can bolster cooperative behavior.[48,49] On the other hand, the qualitative result, i.e., the cooperators have the absolute advantage of being able to dominate the whole population when δ exceeds a critical threshold ($\delta > \delta_{\min}$), is not changed. In brief, these results show that the effect of noise is robust for the system when the individuals are faced with a smaller temptation. Remarkably, similar phenomenon emerges when we examine the system's resilience under a higher temptation factor, specifically for $b = 1.1$, in contrast to the case where $b = 1.02$. In other words, we find that an optimal noise environment can facilitate cooperation under a high temptation level. Namely,

$$\left\{K^{\text{opt}} \middle| 0.1 \le K^{\text{opt}} \le 1.0\right\} = \arg\max_{K\in[0,3]} \rho_c \quad (b = 1.02), \tag{23}$$

$$\left\{K^{\text{opt}} \middle| 0.4 \le K^{\text{opt}} \le 0.5\right\} = \arg\max_{K\in[0,3]} \rho_c \quad (b = 1.10). \tag{24}$$

As a consequence, we believe that the effect of noise is robust in the system for different values of b, although the interval width of K^{opt} gets narrower and narrower with increasing b.

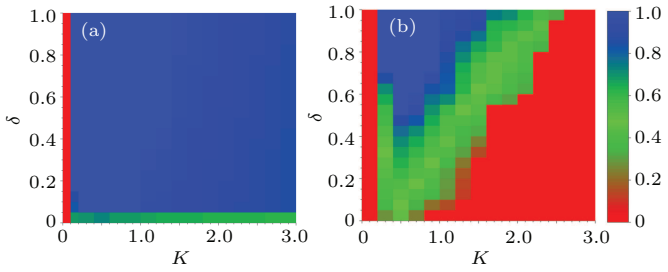


Fig. 7. Density of cooperation ρ_c is influenced by the noise intensity K and the driving coefficient δ. It shows that the qualitative result does not change under the influence of noise whether the temptation value is smaller or bigger, so we believe the system is robust for different values of temptation. (a) For a smaller temptation $b = 1.02$; (b) for a bigger temptation $b = 1.10$. Other relevant parameters: $N = 100$, $m = 2\times10^3$, $T = 10^4$ (even 10^5) and $n = 100$.

We have presented all the experimental results for our computation model and analyzed the cooperative dynamics in the population in detail. However, it is necessary to state that these results are obtained on a 100×100 square lattice with a von Neumann neighborhood. When we adjust the size of lattice, whether for a small-scale network (e.g., 50×50) or a large-scale one (e.g., 200×200), the results obtained are consistent with those in this paper. Also, we tested the evolution of cooperation on a square lattice with a Moore neighborhood and on a scale-free network, respectively. The results show that the qualitative results do not change by comparing them with those presented in foregoing statistics diagrams, although the dependence of ρ_c on b (or δ) is more continuous on such networks. Here, we briefly explain the reason why the results are more continuous on the square lattice with a Moore neighborhood. As is known to all, there are triangular frames in the spatial structure; for full interaction (the interaction intensity between paired individuals is equal to 1), it will lead to the defectors having more opportunities to invade the cooperative cluster. However, when we introduce our mechanism, which is an adaptive interaction driven by the learning effect, the chances of invading are reduced for defectors. On the other hand, the characteristic of high clustering in the lattice promotes the clustering ability of the cooperative cluster. For these reasons, a smaller-scale cooperative cluster can exist and be maintained near the transition point, which reduces fluctuations of the data points. Over the next few years, our research will primarily focus on the cooperative dynamics of adaptive interaction within the context of virus transmission[50–52] in terms of single-layer and multi-layer networks.

5. Conclusion

Within social groups, the connections among individuals are intricately linked to the process of mutual learning. For this reason, we establish a model of self-adapting interaction driven by the learning effect to investigate the evolutionary PDG on a directed and weighted square lattice. In this computation model, a learner is likely to naturally increase the interaction strength directed towards his mentor, whom he mimics, when his cumulative payoff is more than the reference payoff. Conversely, the interaction strength will weaken when the cumulative payoff is less than the reference payoff. Experimental results indicate that the mechanism can drastically improve the cooperation level in the spatial PDG. The parameter δ, which is the driving coefficient of interaction intensity, plays an important role in cooperation within the population. Interestingly, for a certain range of temptations, we notice that cooperators have the absolute advantage of being able to dominate the whole population when δ exceeds a critical threshold. However, for a large uncooperative faction, although the cooperators do not have the advantage of dominating the population, there is still a small driving coefficient $\delta_{\min}$ that can provide a moderate environment for the survival of cooperators. By kinetic analysis, we find that there is a positive feedback effect between an individual's satisfaction frequency and his number of effective neighbors. This positive feedback effect is observably enhanced with increasing δ. Furthermore, we extend the pair-approximation method and apply it to verify the simulation results. The results from the theoretical analysis and the numerical simulation are basically coincident, although there are some subtle differences. Finally, by studying the robustness of the system under the influence of noise, we find that our system is robust under different strengths of social dilemma.

Acknowledgement

Project supported by the National Natural Science Foundation of China (Grant No. 61963013).

References

[1] Allen B, Gore J and Nowak M A 2013 *eLife* **2** e01169
[2] Zhang J L, Chen Z Q and Liu Z X 2016 *Phys. Rev. E* **93** 032320
[3] Radzvilavicius A L, Stewart A J and Plotkin J B 2019 *eLife* **8** e44269
[4] Zhang J L and Zhang C Y 2015 *J. Stat. Mech.* **5** p05001
[5] Hao D, Rong Z H and Zhou T 2014 *Chin. Phys. B* **23** 078905
[6] Wang X J, Gu C L, Lv S J and Quan J 2019 *Chin. Phys. B* **28** 020203
[7] Xiao Y P, Chen D Q, Wei S H, Li Q, Wang H H and Xu M 2019 *Nonlinear Dyn.* **95** 523
[8] Li J Q, Zhang C Y, Sun Q L, Chen Z Q and Zhang J L 2017 *IEEE Trans. Evol. Comput.* **21** 506
[9] Zhang J L, Xu Z M, Liu Z X and Chen Z Q 2018 *Int. J. Syst. Sci* **49** 1934
[10] Tanimoto J An X 2019 *Chaos Soliton Fract.* **122** 1
[11] Sigmund K 2007 *Trends Ecol. Evol.* **22** 593
[12] Zhang J L, Zhang C Y and Cao M 2015 *Sci. Rep.* **5** 9098
[13] Tanimoto J 2014 *Phys. Rev. E* **89** 012106
[14] Santos F C and Pacheco J M 2006 *Proc. Natl. Acad. Sci. USA* **103** 3490
[15] Liu L J, Chen X J and Perc M 2019 *Nonlinear Dyn.* **97** 749
[16] Liang H L, Cui Y, Ren X Q and Wang X F 2021 *Informa. Sciences* **579** 888
[17] Nowak M A and May R M 1992 *Nature* **359** 826
[18] Ariful Kabir K M, Tanimoto J and Wang Z 2018 *Eur. Phys. J. B* **91** 312
[19] Iotti B, Antonioni A, Bullock S, Darabos C, Tomassini M and Giacobini M 2017 *Phys. Rev. E* **96** 052316
[20] Ichinose G and Sayama H 2017 *Artif. Life* **23** 25
[21] Wu Y, Zhang B and Zhang S H 2017 *Chaos Soliton Fract.* **103** 289
[22] Liu J Z, Meng H R, Wang W, Li T and Yu Y 2018 *Chaos Soliton Fract.* **109** 214
[23] Cuesta J A, Gracialázaro C, Ferrer A, Moreno Y and Sánchez A 2015 *Sci. Rep.* **5** 7843
[24] Xia C Y, Wang J, Perc M and Wang Z 2023 *Phys. Life Rev.* **46** 8
[25] Wang J and Xia C Y 2023 *Europhys. Lett.* **141** 21001
[26] Chen M H, Wang L, Sun S W, Wang J and Xia C Y 2016 *Phys. Lett. A* **380** 40
[27] Shen C, Chu C, Shi L, Jusup M, Perc M and Wang Z 2018 *EPL* **124** 48003
[28] Chen X J and Wang L 2009 *Phys. Rev. E* **80** 046109
[29] Szolnoki A and Perc M 2008 *New J. Phys.* **10** 043036
[30] Chen Y Z, Huang Z G, Wang S J, Zhang Y and Wang Y H 2008 *Phys. Rev. E* **79** 055101
[31] Ye W X and Fan S H 2017 *Appl. Math. Comput.* **294** 310
[32] Ye W X, Feng W Y, Lü C and Fan S H 2017 *Appl. Math. Comput.* **307** 31
[33] Gao L, Wang W, Shu P P, Gao H and Braunstein L A 2017 *Europhys. Lett.* **118** 18001
[34] Li J Q, Dang J W and Zhang J L 2020 *Appl. Math. Comput.* **369** 124837
[35] Dai Y Y, Zhan G J, Ye Y, Bao W, Wen T, Cheong K H and Xie N G 2021 *Chaos* **31** 033153
[36] Li J Q, Zhang C Y, Sun Q L and Chen Z Q 2015 *Chaos Soliton Fract.* **77** 253
[37] Li Y, Ye H and Zhang H 2016 *Physica A* **445** 48
[38] Wang Z, Wang L, Szolnoki A and Perc M 2015 *Eur. Phys. J. B* **88** 124
[39] Shi L, Shen C, Geng Y N, Chu C, Meng H R, Perc M, Boccaletti S and Wang Z 2019 *Nonlinear Dyn.* **96** 49
[40] Luo C, Zhang X L and Zheng Y J 2017 *Commun. Nonlinear Sci. Numer. Simul.* **47** 407
[41] Traulsen A, Nowak M A and Pacheco J M 2007 *J. Theor. Biol.* **244** 349
[42] Chen X J, Fu F and Wang L 2008 *Phys. Rev. E* **78** 051120
[43] Li J Q, Park J H, Zhang J L, Chen Z Q and Dehmer M 2020 *Nonlinear Dyn.* **100** 831
[44] Szabó G and Töke C 1998 *Phys. Rev. E* **58** 69
[45] Szabó G and Fath G 2007 *Phys. Rep.* **446** 97
[46] Blume L E 1993 *Games Econ. Behav.* **5** 387
[47] Hauert C and Doebeli M 2004 *Nature* **428** 643
[48] Wang Z and Szolnoki A 2014 *New J. Phys.* **16** 033041
[49] Yang G L, Zhang W M and Xiu B X 2015 *J. Theor. Biol.* **372** 118
[50] Chen Y H and Huang H 2022 *Appl. Math. Comput.* **416** 126754
[51] Xu X L, Chen Z Q, Si G Y, Hu X F, Jiang Y Q and Xu X S 2011 *Nonlinear Dyn.* **64** 117
[52] Xia C Y, Wang L, Sun S and Wang J 2012 *Nonlinear Dyn.* **69** 927